European Radiology (2018) 28:2923–2933
https://doi.org/10.1007/s00330-017-5286-x

HEAD AND NECK

Standard diffusion-weighted, diffusion kurtosis and intravoxel incoherent motion MR imaging of sinonasal malignancies: correlations with Ki-67 proliferation status

Zebin Xiao[1] · Yufeng Zhong[1,2] · Zuohua Tang[1] · Jinwei Qiang[2] · Wen Qian[1] · Rong Wang[1] · Jie Wang[3] · Lingjie Wu[4] · Wenlin Tang[5] · Zhongshuai Zhang[5]

Received: 16 September 2017 / Revised: 11 December 2017 / Accepted: 22 December 2017 / Published online: 30 January 2018

Abstract

Objectives To explore the correlations of parameters derived from standard diffusion-weighted imaging (DWI), diffusion kurtosis imaging (DKI) and intravoxel incoherent motion (IVIM) with the Ki-67 proliferation status.

Methods Seventy-five patients with histologically proven sinonasal malignancies who underwent standard DWI, DKI and IVIM were retrospectively reviewed. The mean, minimum, maximum and whole standard DWI [apparent diffusion coefficient (ADC)], DKI [diffusion kurtosis (K) and diffusion coefficient (Dk)] and IVIM [pure diffusion coefficient (*D*), pseudo-diffusion coefficient (*D**) and perfusion fraction (*f*)] parameters were measured and correlated with the Ki-67 labelling index (LI). The Ki-67 LI was categorised as high (> 50%) or low (≤ 50%).

Results The K and *f* values were positively correlated with the Ki-67 LI (rho = 0.295~0.532), whereas the ADC, Dk and *D* values were negatively correlated with the Ki-67 LI (rho = -0.443~-0.277). The ADC, Dk and *D* values were lower, whereas the K value was higher in sinonasal malignancies with a high Ki-67 LI than in those in a low Ki-67 LI (all $p < 0.05$). A higher maximum K value ($K_{max} > 0.977$) independently predicted a high Ki-67 status [odds ratio (OR) = 7.614; 95% confidence interval (CI) = 2.197-38.674; $p = 0.017$].

Conclusion ADC, Dk, K, *D* and *f* are correlated with Ki-67 LI. K_{max} is the strongest independent factor for predicting Ki-67 status.

Key Points

- *DWI-derived parameters from different models are capable of providing different pathophysiological information.*
- *DWI, DKI and IVIM parameters are associated with Ki-67 proliferation status.*
- *K_{max} derived from DKI is the strongest independent factor for the prediction of Ki-67 proliferation status.*

Keywords Neoplasms · Magnetic resonance imaging · Immunohistochemistry · Diffusion magnetic resonance imaging · Prognosis

Zebin Xiao and Yufeng Zhong contributed equally to this work.

✉ Zuohua Tang
tzh518sunny@163.com

✉ Jinwei Qiang
dr.jinweiqiang@163.com

[1] Department of Radiology, Eye & ENT Hospital of Shanghai Medical School, Fudan University, 83 Fenyang Road, Shanghai 200031, People's Republic of China

[2] Department of Radiology, Jinshan Hospital of Shanghai Medical School, Fudan University, 1508 Longhang Road, Shanghai 201508, People's Republic of China

[3] Department of Radiotherapy, Eye & ENT Hospital of Shanghai Medical School, Fudan University, Shanghai 200031, China

[4] Department of Otolaryngology, Eye & ENT Hospital of Shanghai Medical School, Fudan University, Shanghai 200031, China

[5] Siemens Healthcare Ltd., Shanghai 201318, People's Republic of China

Abbreviations

ADC	Apparent diffusion coefficient
AUC	Area under the curve
CI	Confidence interval
DKI	Diffusion kurtosis imaging
DWI	Diffusion-weighted imaging
EPI	Echo planar imaging
FOV	Field of view
ICC	Intraclass correlation coefficient
IVIM	Intravoxel incoherent motion
LI	Labelling index
NPV	Negative predictive value
OR	Odds ratio
PPV	Positive predictive value
ROC	Receiver-operating characteristic
ROIs	Regions of interest

Introduction

Sinonasal malignancies refer to heterogeneous malignant tumours of epithelial, mesenchymal, neuroendocrine and lymphoid origins in the sinonasal tract [1] and account for approximately 3% of all head and neck tumours [2–4]. Although many treatment alternatives are available in clinical practice, the long-term survival rates associated with these malignancies remain disappointing [5–8]. Comprehensive knowledge of tumour aggressiveness prior to treatment is helpful to predict the prognosis and personalise the treatment for the patients [7, 8]. Tumour proliferation status, which is associated with tumour behaviour, is a promising indicator used to evaluate tumour aggressiveness [7, 8]. The Ki-67 labelling index (LI), which reflects the proliferative activity of the tumour, has been widely used as a prognostic predictor for many malignant tumours, such as gliomas [9], breast carcinomas [10] and olfactory neuroblastoma [11]. Previously, Valente et al. [7] first reported that a high Ki-67 LI with a cut-off value of 50% was positively associated with a poor prognosis in patients with sinonasal carcinomas. Similarly, Airoldi et al. [8] indicated that Ki-67 LI > 50% was a significant predictor of poor overall survival, a high ratio of local relapse or distant metastasis. Hence, the cut-off value of 50% Ki-67 LI has been recommended as a potentially valuable biomarker for predicting the locoregional recurrence, metastasis and prognosis of patients with sinonasal malignancies.

Diffusion-weighted imaging (DWI) with a mono-exponential model, which assumes that water molecule movement follows a Gaussian distribution, is capable of noninvasively reflecting cellularity within lesions using the apparent diffusion coefficient (ADC) value [12]. Previous studies have demonstrated that the ADC value might be a potential indicator for predicting the Ki-67 LI in various tumours, including gliomas [13], breast cancers [14], ovarian tumours [15] and squamous cell carcinomas in the head and the neck [16]. However, given the complex cellular microstructural barriers within tumours, water diffusion behaviour in tumours is considerably more complicated [17]. Therefore, several advanced MR techniques with extended diffusion models, including diffusion kurtosis imaging (DKI) and intravoxel incoherent motion (IVIM), have been proposed to provide a more accurate illumination of the diffusion behaviour of water molecules within tumours [18–20]. For one thing, DKI with a polynomial model (non-Gaussian model) was first proposed by Jensen et al. [18], and this method can more accurately describe the complicated water diffusivity in biological tissue and provide additional information about tissue heterogeneity and cellularity with high *b* values. Yet another IVIM with a bi-exponential model is a method that was initially proposed by Le Bihan et al. [19, 20] to quantitatively assess the microscopic translational motions that occur in each image voxel on MRI, distinguishing both pure molecular diffusion and capillary perfusion with sufficiently low *b* values. Recently, DKI and IVIM have been increasingly used to characterise water diffusion patterns in tumour microstructures involving a variety of tumours in the head and neck [17, 21–26]. More importantly, extended DWI-derived parameters are correlated with the Ki-67 LI in gliomas [13], ovarian tumours [15] and breast cancers [27], revealing that DKI and IVIM may be potentially helpful for predicting the proliferation status of sinonasal malignant tumours.

However, to the best of our knowledge, little is known about the associations between quantitative parameters derived from standard DWI, DKI and IVIM and the Ki-67 LI in sinonasal malignancies. Thus, the purpose of this study was to explore whether these parameters can be used to preoperatively suggest the Ki-67 statuses of these patients.

Materials and methods

Study population

The institutional review board of our hospital approved this retrospective study, and the informed consent requirement was waived because of the retrospective nature of this study. A total of 83 consecutive patients with sinonasal solid masses were recruited between May 2015 and April 2017 based on the following inclusion criteria: (1) malignant tumours were histopathologically proven by surgery/biopsy; (2) standard DWI, DKI and IVIM were performed; (3) an immunohistochemical marker of Ki-67 was available from pathology. The exclusion criteria were as follows: (1) image quality was insufficient because of severe artefacts ($n = 3$); (2) the lesion was too small (< 10 mm in short-axis diameters) ($n = 3$); (3) the patient had a history of treatment or recurrence before MR examinations ($n = 2$). Ultimately, 75 patients (51 males and 24 females; mean age 52.33 ± 17.74 years; range, 23-82 years) with sinonasal

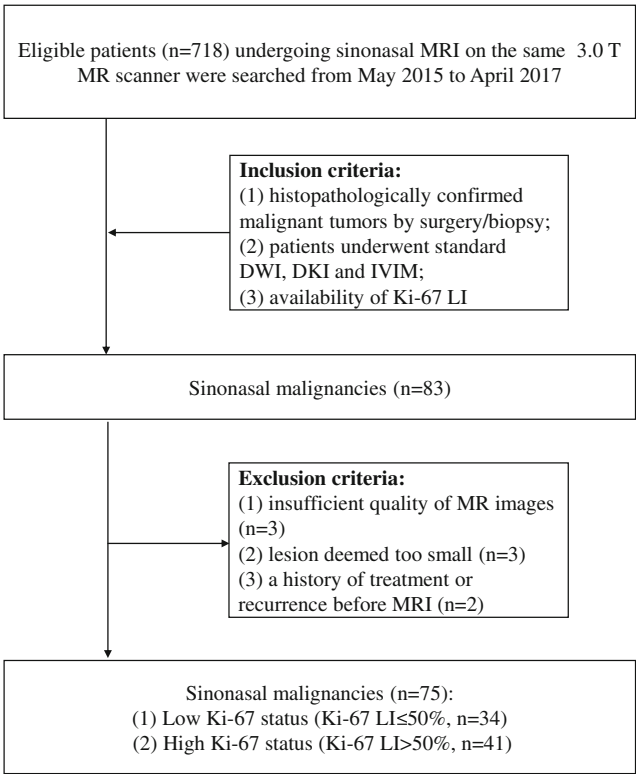

Fig. 1 Flowchart depicting the study selection process

malignant tumours, including squamous cell carcinomas (n = 23), olfactory neuroblastomas (n = 13), malignant melanomas (n = 12), rhabdomyosarcomas (n = 9), malignant lymphomas (n = 6), adenoid cystic carcinomas (n = 5), undifferentiated carcinomas (n = 2), osteosarcomas (n = 2), neuroendocrine carcinomas (n = 2) and malignant fibrohistiocytoma (n = 1), were enrolled in our retrospective study. The flow chart for the enrolment of the study population is shown in Fig. 1.

MR techniques

MRI examinations were performed on a 3-T MR scanner (Magnetom Verio, Siemens Healthineers, Erlangen, Germany) using a 12-channel head matrix coil. Conventional MR sequences were scanned, and then DWI was performed by using a single-shot echo planar imaging (EPI) sequence with a pair of rectangular diffusion gradient pulses along all three orthogonal axes to obtain isotropic DWI images. The imaging parameters were as follows: TR/TE = 5200/83 ms, δ = 27.4 ms, Δ = 39.4 ms, number of averages = 2, acquisition matrix = 120 × 120, field of view (FOV) = 220 mm, slice thickness = 5 mm, intersection gap = 5 mm and parallel imaging acceleration factor = 2. In addition, 14 different b factors ranging from 0 to 2500 s/mm^2 were used (b = 0, 50, 100, 150, 200, 250, 300, 350, 400, 800, 1000, 1500, 2000 and 2500 s/mm^2). The total scan time was 6 min 42 s.

Image processing and analysis

Standard mono-exponential DWI is expressed by the following equation [12]: $S_b/S_0 = \exp(-b\cdot ADC)$, where S_b and S_0 are the signal intensities in the diffusion gradient factors of b and 0, respectively. ADC can be calculated by fitting the signal with b values of 0 and 1000 s/mm^2 to this model. DWI processing was performed on an off-line workstation (Syngo; Siemens Healthineers, Erlangen, Germany). Using the signal intensities of six b-values (b = 0, 400, 800, 1000, 2000 and 2500 s/mm^2), DKI parameters, including Dk and K, can be obtained with the following equation [18]:

$$S_b/S_0 = \exp\left(-b\cdot Dk + b^2\cdot Dk^2\cdot K/6\right), \quad (1)$$

where S_b and S_0 are the signal intensities acquired with the diffusion gradient factors of b and 0, respectively. Dk represents the corrected ADC, and K is the diffusion kurtosis. The IVIM model is expressed as follows [19, 20]:

$$S_b/S_0 = (1-f)\ \exp(-b\cdot D) + f\ \exp\left[-b\cdot\left(D + D^*\right)\right], \quad (2)$$

where S_b and S_0 are the signal intensities in the diffusion gradient factors of b and 0, respectively. Three parameters, D, D^* and f, can be derived from IVIM by fitting MR signal acquired at 11 b-values (b = 0, 50, 100, 150, 200, 250, 300, 350, 400, 800 and 1000 s/mm^2) to a bi-exponential model. f is the perfusion fraction, D is the diffusion coefficient representing pure molecular diffusion, and D^* is the pseudo-diffusion coefficient representing incoherent microcirculation within the voxel.

The mean value of signal intensity distribution within the ROIs was calculated for each b value. Then, the mean signal intensities of b values in Eqs. (1) and (2) were fitted with the least square method using the Levenberg-Marquardt algorithm. For the DKI model, direct fitting to Eq. (1) was performed. As for the IVIM model, a two-step fitting method was used to calculate the increase in the robustness of the fitting with less calculation error as follows: (1) the data of b > 400 s/mm^2 were fitted for the single parameter D, because D^* is significantly larger than D; thus, the influence of pseudo-diffusion on signal decay can be neglected when the b value is greater than 400 s/mm^2 [28]. (2) The curve was fitted for f and D^* over all b values using a nonlinear regression algorithm, while keeping D constant. The Dk, K, D, D^* and f maps were then obtained to calculate IVIM and DKI parameters on a pixel-by-pixel basis. For each pixel, the upper and lower limits were set for f and D^* values to exclude unrealistic measurements and avoid including any erroneous pixels in the calculation. The lower and upper limits of f and D^* were respectively set at 0%-40% and 0–50 × 10^{-3} mm^2/s by referring to the range of each parameter in an earlier report [29]. Additionally, to assess the goodness of fit in both the IVIM and DKI fittings, the coefficient of determination in each pixel was calculated with the following equation: $R^2 = 1 - ESS/TSS$, where ESS is the sum of the squared errors between

the data points and IVIM/DKI fitting curve, and TSS is the sum of the squared differences between the data points and the mean value of all data points. When a pixel's R^2 value was < 0.8, the pixel was excluded from the parameter calculation [30]. DKI and IVIM processing was conducted using MATLAB (version 7.9, MathWorks, Inc., Natick, MA).

Standard DWI (ADC), DKI (Dk and K) and IVIM (*D*, *D** and *f*) parameters were measured independently by two radiologists (readers 1 and 2 with 7 years of experience in head and neck imaging) who were blinded to clinical and histopathological data. Five small round regions of interest with the same size (ROIs; mean area, 34.23 mm^2; range, 30-50 mm^2) were placed inside the tumours on the corresponding parameter maps, which were proposed in a previous study [31]. Consequently, the mean, minimum and maximum ADC (ADC_{mean}, ADC_{min}, and ADC_{max}), Dk (Dk_{mean}, Dk_{min}, and Dk_{max}), K (K_{mean}, K_{min}, and K_{max}), *D* (D_{mean}, D_{min}, and D_{max}), *D** (D^*_{mean}, D^*_{min}, and D^*_{max}) and *f* (f_{mean}, f_{min}, and f_{max}) values were calculated. Moreover, one polygonal ROI (mean area, 177.113 ± 98.106 mm^2; range, 29-776 mm^2) was also drawn along the outer margin of the lesion on the largest slice of the corresponding parameter maps to calculate the standard DWI, DKI and IVIM parameters for the whole lesion, which were referred as ADC_{whole}, Dk_{whole}, K_{whole}, D_{whole}, D^*_{whole} and f_{whole}. Care was taken to avoid haemorrhagic, necrotic, cystic or apparent blood vessel regions by referring to T2-weighted and contrast-enhanced T1-weighted imaging. The measurements made by readers 1 and 2 were used to evaluate the inter-reader reproducibility and were averaged for statistical analysis. To evaluate the intra-reader reproducibility, these measurements were repeated by reader 1, with a minimum washout period of at least 1 month.

Immunohistochemical analysis of the Ki-67 labelling index

Immunohistochemistry of Ki-67 was performed using a commercially available Ki-67 mouse monoclonal antihuman antibody (MIB-1, ZSGBBIO, Beijing, China). Ki-67 analyses were retrospectively performed by a pathologist (21 years of experience in sinonasal pathology) who was blinded to the clinicopathological and MR information. The Ki-67 LI was determined using the percentile of immunoreactive cells from 1000 malignant cells (× 400), and scoring was performed in the areas with the highest number of positive nuclei (hot spot) within the tumour. Sinonasal malignant tumours were classified as either low (Ki-67 LI ≤ 50%) or high Ki-67 status (Ki-67 LI > 50%) in our study [7, 8].

Statistical analysis

All standard DWI, DKI and IVIM parameters of sinonasal malignancies were presented as the means ± standard deviation. The inter- and intra-reader reproducibility for parameter measurements was evaluated using the intraclass correlation coefficient (ICC) with 95% confidence intervals (CI). An ICC > 0.75 was considered indicative of good agreement. Spearman correlations were used to characterise the correlations among the standard DWI, DKI and IVIM parameters and the Ki-67 LI of the individual lesions. A correlation coefficient rho (*r*) of 0.75-1.00 was deemed to indicate very good to excellent correlation; 0.50-0.74, moderate to good correlation; 0.25-0.49, fair correlation; 0.24 or lower, little or no correlation. Comparisons of the standard DWI, DKI and IVIM parameters for tumours with low and high Ki-67 expression were made with the Student's *t*-tests. $p < 0.05$ was considered statistically significant. Receiver-operating characteristic (ROC) curve analyses were calculated to determine the optimal cut-off value for significant parameters for differentiating between low and high Ki-67 status. The area under the curve (AUC), Youden index, sensitivity, specificity, accuracy, positive predictive value (PPV) and negative predictive value (NPV) of these parameters for differential diagnosis were calculated. The parameters with the highest Youden index were enrolled into multivariate logistic regression analysis to explore the associations between quantitative MR parameters and a high Ki-67 status. Statistical analyses were performed using Excel 2013 (Microsoft, Redmond, WA) and MedCalc statistical software (version 15.2.2, Ostend, Belgium).

Results

As shown in Table 1, good inter- and intra-reader agreements were achieved for the measurement of the ROI size, standard DWI, IVIM and DKI parameters (ICC ranging from 0.761 to 0.944). The Ki-67 LI of the lesions ranged from 2% to 90% with a mean of 54.55%. The correlations between quantitative MR parameters (ADC, Dk, K, *D*, *D** and *f*) and the Ki-67 LI in malignant sinonasal tumours are summarised in Table 2. The K_{mean}, K_{min}, K_{max}, K_{whole}, f_{max} and f_{whole} values were positively correlated with the Ki-67 LI (r = 0.493, 0.401, 0.532, 0.453, 0.382 and 0.295, respectively; all $p < 0.05$), whereas the ADC_{mean}, ADC_{min}, ADC_{max}, ADC_{whole}, Dk_{mean}, Dk_{min}, Dk_{max}, Dk_{whole}, D_{mean}, D_{min}, D_{max} and D_{whole} values were negatively correlated with the Ki-67 LI (r = -0.372, -0.443, -0.364, -0.411, -0.360, -0.388, -0.277, -0.294, -0.374, -0.401, -0.304 and -0.376, respectively; all $p < 0.05$).

Table 3 presents the results of the comparative analyses of ADC, Dk, K, *D*, *D** and *f* between low and high Ki-67 statuses in sinonasal malignant tumours. The mean ADC_{mean}, ADC_{min}, ADC_{max}, ADC_{whole}, Dk_{mean}, Dk_{min}, Dk_{max}, Dk_{whole}, D_{mean}, D_{min}, D_{max} and D_{whole} values were significantly lower with a high Ki-67 status than those with a low Ki-67 status in sinonasal malignancies (all $p < 0.05$), whereas the mean K_{mean}, K_{min}, K_{max} and K_{whole} values of sinonasal

Table 1 The inter- and intra-reader reproducibility for ROI size, ADC, Dk, K, *D*, *D** and *f* measurements

Parameters	ICC (95% CI)	
	Inter-reader	Intra-reader
ROI size measurement		
Small round ROI	0.932 (0.897-0.995)	0.944 (0.901-1.000)
Polygonal ROI	0.918 (0.884-0.973)	0.902 (0.846-0.978)
Standard DWI parameters		
ADC_{mean} ($\times 10^{-3}$ mm^2/s)	0.875 (0.792-0.933)	0.822 (0.750-0.941)
ADC_{min} ($\times 10^{-3}$ mm^2/s)	0.829 (0.764-0.901)	0.833 (0.762-0.909)
ADC_{max} ($\times 10^{-3}$ mm^2/s)	0.791 (0.704-0.935)	0.773 (0.726-0.851)
ADC_{whole} ($\times 10^{-3}$ mm^2/s)	0.920 (0.835-0.966)	0.901 (0.854-0.979)
DKI parameters		
Dk_{mean} ($\times 10^{-3}$ mm^2/s)	0.874 (0.778-0.942)	0.858 (0.731-0.924)
Dk_{min} ($\times 10^{-3}$ mm^2/s)	0.823 (0.754-0.885)	0.874 (0.800-0.931)
Dk_{max} ($\times 10^{-3}$ mm^2/s)	0.837 (0.781-0.905)	0.895 (0.810-0.937)
Dk_{whole} ($\times 10^{-3}$ mm^2/s)	0.894 (0.815-0.962)	0.886 (0.804-0.952)
K_{mean}	0.902 (0.859-0.971)	0.890 (0.841-0.953)
K_{min}	0.873 (0.806-0.941)	0.892 (0.820-0.944)
K_{max}	0.850 (0.812-0.900)	0.904 (0.859-0.969)
K_{whole}	0.933 (0.881-0.977)	0.904 (0.853-0.953)
IVIM parameters		
D_{mean} ($\times 10^{-3}$ mm^2/s)	0.815 (0.755-0.892)	0.812 (0.751-0.953)
D_{min} ($\times 10^{-3}$ mm^2/s)	0.891 (0.812-0.931)	0.915 (0.883-0.968)
D_{max} ($\times 10^{-3}$ mm^2/s)	0.761 (0.721-0.840)	0.774 (0.729-0.799)
D_{whole} ($\times 10^{-3}$ mm^2/s)	0.886 (0.833-0.920)	0.870 (0.844-0.907)
D^*_{mean} ($\times 10^{-3}$ mm^2/s)	0.791 (0.747-0.833)	0.822 (0.790-0.841)
D^*_{min} ($\times 10^{-3}$ mm^2/s)	0.797 (0.731-0.850)	0.775 (0.729-0.827)
D^*_{max} ($\times 10^{-3}$ mm^2/s)	0.812 (0.785-0.901)	0.863 (0.802-0.912)
D^*_{whole} ($\times 10^{-3}$ mm^2/s)	0.844 (0.805-0.877)	0.832 (0.788-0.860)
f_{mean} (%)	0.891 (0.817-0.933)	0.922 (0.817-0.993)
f_{min} (%)	0.907 (0.731-0.850)	0.924 (0.823-0.961)
f_{max} (%)	0.885 (0.821-0.944)	0.856 (0.802-0.930)
f_{whole} (%)	0.901 (0.854-0.986)	0.897 (0.858-0.957)

ICC, intraclass correlation coefficient; 95% CI, 95% confidence intervals; ADC, apparent diffusion coefficient; ADC_{mean}, mean ADC; ADC_{min}, minimum ADC; ADC_{max}, maximum ADC; ADC_{whole}, ADC for the whole lesion; Dk, diffusion coefficient; Dk_{mean}, mean Dk; Dk_{min}, minimum Dk; Dk_{max}, maximum Dk; Dk_{whole}, Dk for the whole lesion; K, diffusion kurtosis; K_{mean}, mean K; K_{min}, minimum K; K_{max}, maximum K; K_{whole}, K for the whole lesion; *D*, pure diffusion coefficient; D_{mean}, mean *D*; D_{min}, minimum *D*; D_{max}, maximum *D*; D_{whole}, *D* for the whole lesion; *D**, pseudo-diffusion coefficient; D^*_{mean}, mean *D**; D^*_{min}, minimum *D**; D^*_{max}, maximum *D**; D^*_{whole}, *D** for the whole lesion; *f*, perfusion fraction; f_{mean}, mean *f*; f_{min}, minimum *f*; f_{max}, maximum *f*; f_{whole}, *f* for the whole lesion

Table 2 Correlations between quantitative MR parameters (ADC, Dk, K, *D*, *D** and *f*) and the Ki-67 labelling index in malignant sinonasal tumours

Parameters	Ki-67 Labelling Index	
	r (95% CI)	*p* value
Standard DWI parameters		
ADC_{mean} ($\times 10^{-3}$ mm^2/s)	-0.372 (-0.611, -0.106)	0.002
ADC_{min} ($\times 10^{-3}$ mm^2/s)	-0.443 (-0.579, -0.147)	< 0.001
ADC_{max} ($\times 10^{-3}$ mm^2/s)	-0.364 (-0.589, -0.109)	0.001
ADC_{whole} ($\times 10^{-3}$ mm^2/s)	-0.411 (-0.625, -0.177)	< 0.001
DKI parameters		
Dk_{mean} ($\times 10^{-3}$ mm^2/s)	-0.360 (-0.571, -0.223)	0.003
Dk_{min} ($\times 10^{-3}$ mm^2/s)	-0.388 (-0.745, -0.179)	0.001
Dk_{max} ($\times 10^{-3}$ mm^2/s)	-0.277 (-0.486, 0.012)	0.038
Dk_{whole} ($\times 10^{-3}$ mm^2/s)	-0.294 (-0.556, 1.033)	0.035
K_{mean}	0.493 (0.142, 0.643)	< 0.001
K_{min}	0.401 (0.117, 0.775)	< 0.001
K_{max}	0.532 (0.209, 0.738)	< 0.001
K_{whole}	0.453 (0.162, 0.791)	< 0.001
IVIM parameters		
D_{mean} ($\times 10^{-3}$ mm^2/s)	-0.374 (-0.739, -0.198)	0.006
D_{min} ($\times 10^{-3}$ mm^2/s)	-0.401 (-0.459, 0.137)	0.001
D_{max} ($\times 10^{-3}$ mm^2/s)	-0.304 (-0.595, -0.090)	0.005
D_{whole} ($\times 10^{-3}$ mm^2/s)	-0.376 (-0.771, 0.233)	0.007
D^*_{mean} ($\times 10^{-3}$ mm^2/s)	0.201 (-0.199, 0.453)	0.212
D^*_{min} ($\times 10^{-3}$ mm^2/s)	-0.104 (-0.536, 0.251)	0.486
D^*_{max} ($\times 10^{-3}$ mm^2/s)	-0.088 (-0.370, 0.265)	0.802
D^*_{whole} ($\times 10^{-3}$ mm^2/s)	-0.112 (-0.455, 0.359)	0.662
f_{mean} (%)	0.103 (-0.110, 0.481)	0.141
f_{min} (%)	0.226 (-0.145, 0.561)	0.084
f_{max} (%)	0.382 (0.139, 0.669)	0.033
f_{whole} (%)	0.295 (0.114, 0.734)	0.039

r, correlation coefficient; 95% CI, 95% confidence intervals; ADC, apparent diffusion coefficient; ADC_{mean}, mean ADC; ADC_{min}, minimum ADC; ADC_{max}, maximum ADC; ADC_{whole}, ADC for the whole lesion; Dk, diffusion coefficient; Dk_{mean}, mean Dk; Dk_{min}, minimum Dk; Dk_{max}, maximum Dk; Dk_{whole}, Dk for the whole lesion; K, diffusion kurtosis; K_{mean}, mean K; K_{min}, minimum K; K_{max}, maximum K; K_{whole}, K for the whole lesion; *D*, pure diffusion coefficient; D_{mean}, mean *D*; D_{min}, minimum *D*; D_{max}, maximum *D*; D_{whole}, *D* for the whole lesion; *D**, pseudo-diffusion coefficient; D^*_{mean}, mean *D**; D^*_{min}, minimum *D**; D^*_{max}, maximum *D**; D^*_{whole}, *D** for the whole lesion; *f*, perfusion fraction; f_{mean}, mean *f*; f_{min}, minimum *f*; f_{max}, maximum *f*; f_{whole}, *f* for the whole lesion

malignancies with a high Ki-67 status were significantly higher than those of sinonasal malignancies with a low Ki-67 status (all $p < 0.05$) (Figs. 2 and 3).

As demonstrated in Table 4, the four MR parameters, including the ADC (ADC_{mean}, ADC_{min}, ADC_{max} and ADC_{whole}), Dk (Dk_{mean}, Dk_{min}, Dk_{max} and Dk_{whole}), K (K_{mean}, K_{min}, K_{max} and K_{whole}) and *D* (D_{mean}, D_{min}, D_{max} and D_{whole}) values, were useful for the differentiation of low and high Ki-67 statuses in sinonasal malignant neoplasms with similar diagnostic performances (AUC ranging from 0.644 to 0.742; all $p > 0.05$ compared with each other). Four variables with the highest Youden index were included in the multivariate analysis, demonstrating

Table 3 Comparison of ADC, Dk, K, *D*, *D** and *f* values of malignant sinonasal tumours with low and high Ki-67 statuses (mean ± SD)

Parameters	Low Ki-67 status (n = 34)	High Ki-67 status (n = 41)	p value
Standard DWI parameters			
ADC_{mean} (× 10^{-3} mm^2/s)	1.097 ± 0.243	0.815 ± 0.235	0.003
ADC_{min} (× 10^{-3} mm^2/s)	1.001 ± 0.361	0.798 ± 0.220	0.001
ADC_{max} (× 10^{-3} mm^2/s)	1.187 ± 0.302	0.927 ± 0.229	0.004
ADC_{whole} (× 10^{-3} mm^2/s)	0.994 ± 0.285	0.805 ± 0.221	0.002
DKI parameters			
Dk_{mean} (× 10^{-3} mm^2/s)	1.385 ± 0.330	1.136 ± 0.292	0.008
Dk_{min} (× 10^{-3} mm^2/s)	1.328 ± 0.351	1.110 ± 0.397	0.005
Dk_{max} (× 10^{-3} mm^2/s)	1.413 ± 0.337	1.249 ± 0.272	0.027
Dk_{whole} (× 10^{-3} mm^2/s)	1.325 ± 0.352	1.125 ± 0.203	0.009
K_{mean}	0.900 ± 0.239	1.060 ± 0.243	0.005
K_{min}	0.887 ± 0.228	1.091 ± 0.221	< 0.001
K_{max}	0.956 ± 0.221	1.311 ± 0.230	< 0.001
K_{whole}	0.909 ± 0.235	1.085 ± 0.236	0.002
IVIM parameters			
D_{mean} (× 10^{-3} mm^2/s)	0.659 ± 0.185	0.550 ± 0.123	0.003
D_{min} (× 10^{-3} mm^2/s)	0.561 ± 0.174	0.436 ± 0.117	0.001
D_{max} (× 10^{-3} mm^2/s)	0.765 ± 0.168	0.625 ± 0.150	0.006
D_{whole} (× 10^{-3} mm^2/s)	0.641 ± 0.173	0.538 ± 0.119	0.003
D^*_{mean} (× 10^{-3} mm^2/s)	38.342 ± 24.187	41.799 ± 17.340	0.910
D^*_{min} (× 10^{-3} mm^2/s)	32.543 ± 20.174	36.231 ± 18.871	0.831
D^*_{max} (× 10^{-3} mm^2/s)	41.325 ± 19.736	44.205 ± 20.343	0.795
D^*_{whole} (× 10^{-3} mm^2/s)	47.481 ± 21.659	49.316 ± 13.575	0.633
f_{mean} (%)	17.888 ± 8.586	20.259 ± 9.351	0.260
f_{min} (%)	15.623 ± 4.952	17.503 ± 4.604	0.093
f_{max} (%)	19.329 ± 5.287	21.381 ± 4.772	0.112
f_{whole} (%)	19.034 ± 5.167	20.312 ± 5.638	0.065

ADC, apparent diffusion coefficient; ADC_{mean}, mean ADC; ADC_{min}, minimum ADC; ADC_{max}, maximum ADC; ADC_{whole}, ADC for the whole lesion; Dk, diffusion coefficient; Dk_{mean}, mean Dk; Dk_{min}, minimum Dk; Dk_{max}, maximum Dk; Dk_{whole}, Dk for the whole lesion; K, diffusion kurtosis; K_{mean}, mean K; K_{min}, minimum K; K_{max}, maximum K; K_{whole}, K for the whole lesion; *D*, pure diffusion coefficient; D_{mean}, mean *D*; D_{min}, minimum *D*; D_{max}, maximum *D*; D_{whole}, *D* for the whole lesion; *D**, pseudo-diffusion coefficient; D^*_{mean}, mean *D**; D^*_{min}, minimum *D**; D^*_{max}, maximum *D**; D^*_{whole}, *D** for the whole lesion; *f*, perfusion fraction; f_{mean}, mean *f*; f_{min}, minimum *f*; f_{max}, maximum *f*; f_{whole}, *f* for the whole lesion

that a higher K_{max} value [> 0.984; odds ratio (OR): 8.370, 95% CI: 2.197-38.674; $p = 0.025$] remained independently associated with a high Ki-67 status (Table 5).

Discussion

Ki-67 proliferation status is predominantly assessed by the pathological analysis of biopsy or surgical specimens. The ADC value derived from standard DWI is a useful clinical biomarker for predicting tumour proliferation status [13–16]. The negative correlation between ADC values and tumour cellularity or the Ki-67 LI in a majority of tumours has been widely reported in previous studies [13–16]. However, the complicated microstructures in biological tissues, such as membranes, myelin sheaths and neural axons, can greatly influence water diffusion within the tissues, suggesting that it is inappropriate to interpret water diffusion using a mono-exponential Gaussian model [12, 18–20, 32]. In our current study, DWI was performed in patients with sinonasal malignancies using an extended *b*-value ranging from 0 to 2500 s/mm^2, and the diffusion-weighted signal decay was analysed by using mono-, bi-exponential and polynomial models. Then, the correlations of quantitative parameters derived from standard DWI, DKI and IVIM with the Ki-67 proliferation status were explored in our study.

The results of the present study demonstrated that ADC (ADC_{mean}, ADC_{min}, ADC_{max} and ADC_{whole}), Dk (Dk_{mean}, Dk_{min}, Dk_{max} and Dk_{whole}) and *D* (D_{mean}, D_{min}, D_{max} and D_{whole}) were inversely correlated with the Ki-67 LI, whereas

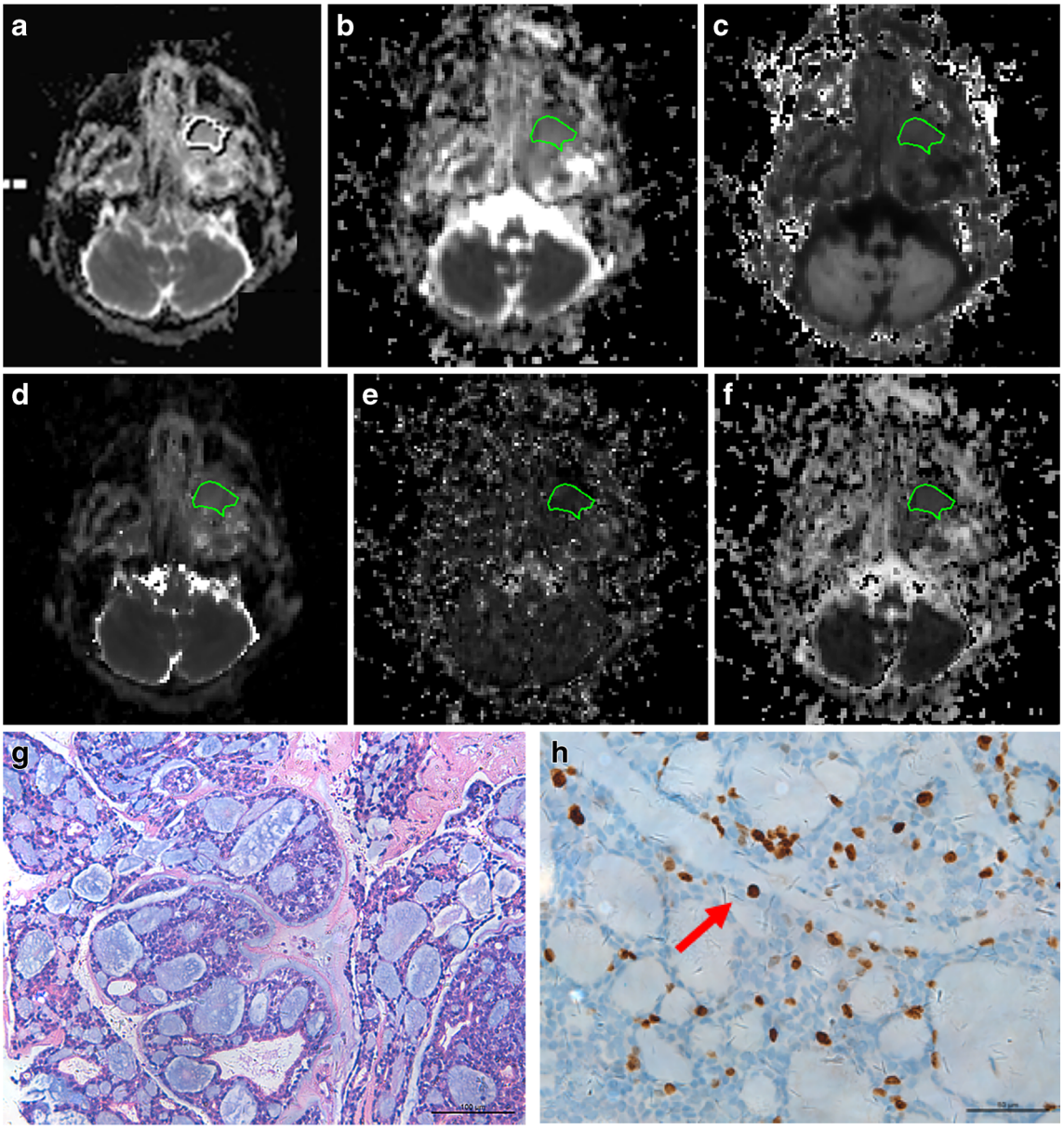

Fig. 2 Adenoid cystic carcinoma in a 47-year-old male. **(a)** An axial ADC map indicates that a hyperintense solid mass is predominantly located in the left maxillary sinus and nasal cavity with the involvement of the pterygopalatine fossa (white polygon ROI) and an ADC value of 1.414×10^{-3} mm^2/s. **(b-c)** The solid component of the mass (green polygon ROI) is hyperintense on the Dk map **(b)** and hypointense on the K map **(c)**, with values of 1.764×10^{-3} mm^2/s and 0.657, respectively. **(d-f)** The solid component of the mass (green polygon ROI) is hyperintense on the *D* map **(d)**, isointense on the *D** map **(e)** and hyperintense on the *f* map **(f)**, with values of 0.887×10^{-3} mm^2/s, 42.673×10^{-3} mm^2/s and 23.375%, respectively. **(g)** Haematoxylin-eosin staining confirms the mass as an adenoid cystic carcinoma (magnification, × 200; scale bar, 100 μm). **(h)** Ki-67 immunohistochemical labelling depicts that approximately 5% of cells are positive for nuclear staining (red arrow; magnification, × 400; scale bar, 50 μm)

K (K_{mean}, K_{min}, K_{max} and K_{whole}) and *f* (f_{max} and f_{whole}) were positively correlated with the Ki-67 LI. As clarified in previous studies, Dk derived from DKI is the corrected diffusion coefficient for non-Gaussian bias [18], whereas *D* derived from IVIM is the pure molecular diffusion coefficient without microcirculation contributions [19, 20]. Thus, it was not surprising that a negative correlation existed between diffusion-related parameters and the Ki-67 LI, because a high level of Ki-67 expression could have an impact on the restriction of water diffusion and therefore can be reflected by decreasing Dk and *D* values in addition to the ADC value. Additionally, malignant sinonasal tumours are typically associated with active neoangiogenesis and complex microstructures within the tumours [7]. However, the *f* value, which measured the fractional volume of capillary blood flowing in each voxel [33, 34], demonstrated little or no positive correlation with the

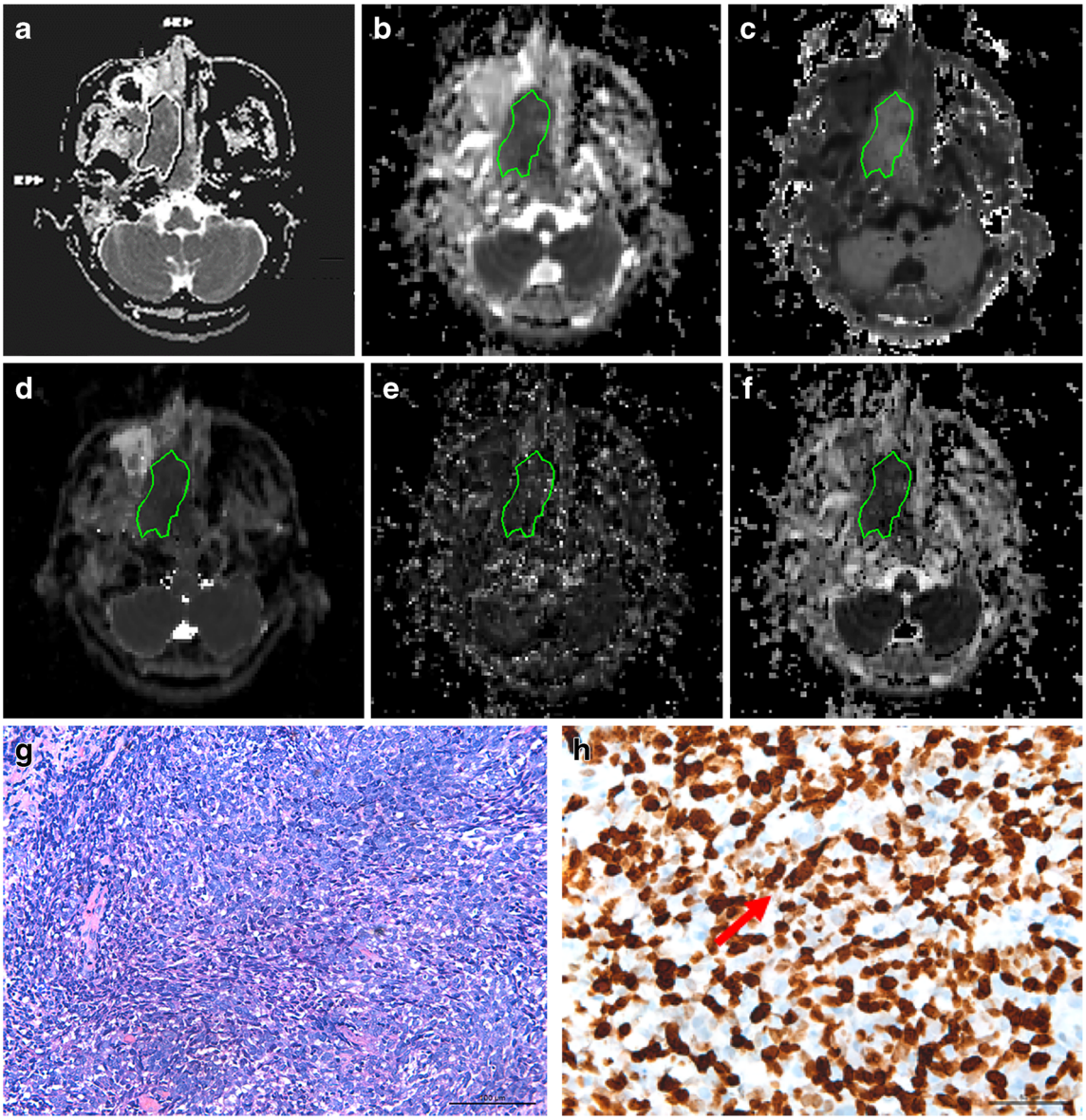

Fig. 3 Squamous cell carcinoma in a 53-year-old male. **(a)** An axial ADC map demonstrates that a heterogeneously hypo- to isointense solid mass is primarily located in the right nasal cavity and posterior naris (white polygon ROI), with an ADC value of 0.751×10^{-3} mm^2/s. **(b-c)** The solid component of the mass (green polygon ROI) is heterogeneously iso- to hyperintense on the Dk map **(b)** and hyperintense on the K map **(c)**, with values of 1.087×10^{-3} mm^2/s and 1.085, respectively. **(d-f)** The solid component of the mass (green polygon ROI) is homogeneously isointense on the *D* map **(d)**, heterogeneously iso- to hyperintense on the *D** map **(e)** and heterogeneously hyperintense on the *f* map **(f)**, with values of 0.517×10^{-3} mm^2/s, 47.342×10^{-3} mm^2/s and 17.131%, respectively. **(g)** Haematoxylin-eosin staining confirms the mass as a squamous cell carcinoma (magnification, × 200; scale bar, 100 μm). **(h)** Ki-67 immunohistochemical labelling reveals that approximately 80% of cells are positive for nuclear staining (red arrow; magnification, × 400; scale bar, 50 μm)

level of Ki-67 expression in this present study, which was not in accordance with previous studies [7, 8], probably because of the heterogeneous patient cohort in our study. Specifically, some sinonasal malignancies, such as olfactory neuroblastomas with abundant microcapillary perfusion (mean *f* = 26.41%), can show a low Ki-67 LI (mean Ki-67 Li = 36.69%), whereas malignant lymphomas can exhibit a low perfusion (mean *f* = 21.16%) and a high Ki-67 LI (mean Ki-67 Li = 75.33%). Moreover, the K value derived from DKI quantifies the deviation of tissue water molecule diffusion from a Gaussian distribution and reflects the complexity or heterogeneity of the tumours. Of note, the K value with the highest *r* among all the parameters was positively correlated with Ki-67 expression, demonstrating that the K value could be a promising parameter for predicting the proliferation status of sinonasal malignant tumours. This finding may be attributed to the fact that the present patient cohort included heterogeneous malignancies in the sinonasal area. Li et al. [15] found that the K value was positively correlated with Ki-67 expression in ovarian tumours, whereas the Dk and ADC

Table 4 Measurements of the threshold value, sensitivity, specificity, PPV, NPV, accuracy and AUC of the ADC, Dk, K and *D* values for differentiating low and high Ki-67 statuses

	TV	Youden index	Sensitivity (%)	Specificity (%)	PPV (%)	NPV (%)	Accuracy (%)	AUC
ADC_{mean}	0.981	0.378	87.8	50.0	67.9	77.3	70.7	0.700
ADC_{min}	0.953	0.402	90.2	50.0	68.5	81.0	72.0	0.716
ADC_{max}	0.995	0.378	87.8	50.0	67.9	77.3	70.7	0.676
ADC_{whole}	0.977	0.402	90.2	50.0	68.5	81.0	72.0	0.703
Dk_{mean}	1.239	0.320	73.2	58.8	68.2	64.5	66.7	0.682
Dk_{min}	1.174	0.344	75.6	58.8	68.9	66.7	68.0	0.690
Dk_{max}	1.372	0.319	87.8	44.1	65.5	75.0	68.0	0.644
Dk_{whole}	1.336	0.320	73.2	58.8	68.2	64.5	66.7	0.677
K_{mean}	0.917	0.408	73.2	67.6	73.2	67.6	70.7	0.738
K_{min}	0.824	0.319	87.8	44.1	65.5	75.0	68.0	0.685
K_{max}	0.984	0.418	82.9	58.8	70.8	74.1	72.0	0.742
K_{whole}	0.977	0.359	68.3	67.6	71.8	63.9	68.0	0.710
D_{mean}	0.563	0.384	70.7	67.6	72.5	65.7	69.3	0.689
D_{min}	0.505	0.397	92.7	47.1	67.9	84.2	72.0	0.702
D_{max}	0.658	0.364	65.9	70.6	73.0	63.2	68.0	0.681
D_{whole}	0.586	0.349	73.2	61.8	69.8	65.6	68.0	0.683

TV, threshold value; PPV, positive predictive value; NPV, negative predictive value; AUC, area under the curve; ADC, apparent diffusion coefficient; ADC_{mean}, mean ADC; ADC_{min}, minimum ADC; ADC_{max}, maximum ADC; ADC_{whole}, ADC for the whole lesion; Dk, diffusion coefficient; Dk_{mean}, mean Dk; Dk_{min}, minimum Dk; Dk_{max}, maximum Dk; Dk_{whole}, Dk for the whole lesion; K, diffusion kurtosis; K_{mean}, mean K; K_{min}, minimum K; K_{max}, maximum K; K_{whole}, K for the whole lesion; *D*, pure diffusion coefficient; D_{mean}, mean *D*; D_{min}, minimum *D*; D_{max}, maximum *D*; D_{whole}, *D* for the whole lesion

values were negatively correlated with Ki-67 expression, which was in accordance with our results. However, in our present study, no correlation was noted between the *D** value and Ki-67 expression. This result was consistent with the findings from a previous study by Yan et al. [13], which demonstrated that *D** (also known as Dfast) was not correlated with Ki-67 expression in gliomas. These phenomena may be caused by the low signal-to-noise ratio and the relatively poor measurement reproducibility of *D** [35].

In addition, we found that sinonasal malignancies with high Ki-67 status exhibited lower ADC, Dk and *D* values but higher K values than those with low Ki-67 status. However, no significant differences in the mean *D** and *f* values were noted between the two groups, because little or no correlation between *f* and the Ki-67 LI was found in our study, and malignant tumours with different proliferation statuses may manifest similar microcapillary perfusion. Regardless, our results suggested that diffusion- (ADC, Dk and *D*) and kurtosis-related (K) parameters may be valuable for the prediction of a high Ki-67 status, whereas perfusion-related parameters (*D** and *f*) were of limited value. Moreover, ADC, Dk, K and *D* exhibited similar diagnostic performances for differentiating high from low Ki-67 statuses. Furthermore, multivariate analysis revealed that a higher K_{max} value was the independent factor associated with a high Ki-67 LI, likely because the microstructure of a sinonasal malignant tumour with a high Ki-67 LI is very complex and therefore can be reflected by the K_{max} value [15, 18, 26, 27]. Hence, K facilitates the identification of highly proliferative tumours, as indicated by the Ki-67 LI, which is meaningful for preoperatively determining the tumour grade and treatment choices as well as predicting responses to treatment and prognosis. In

Table 5 Multivariate logistic regression analysis of quantitative MR parameters (ADC_{min}, Dk_{min}, K_{max} and D_{min}) associated with a high Ki-67 status

Parameters	OR	95% CI	*p* value
ADC_{min} (≤ 0.953 vs. > 0.953) (× 10^{-3} mm^2/s)	4.104	1.784, 9.677	0.237
Dk_{min} (≤ 1.174 vs. > 1.174) (× 10^{-3} mm^2/s)	1.895	0.273, 8.102	0.336
K_{max} (> 0.984 vs. ≤ 0.984)	8.370	2.197, 38.674	0.025
D_{min} (≤ 0.505 vs. > 0.505) (× 10^{-3} mm^2/s)	4.008	0.984, 30.255	0.114

OR, odds ratio; 95% CI, 95% confidence interval; ADC_{min}, minimum apparent diffusion coefficient; Dk_{min}, minimum diffusion coefficient; K_{max}, maximum diffusion kurtosis; D_{min}, minimum pure diffusion coefficient

contrast, ADC, Dk and *D* were not independent predictors for outcomes on multivariate analysis in our present study, which was consistent with the findings reported by Shin et al. [14], demonstrating that ADC was not independently associated with Ki-67 expression. Given that ADC, Dk or *D* was highly correlated with histopathologically prognostic factors, such as histological types and clinical staging of the tumours [14], the independent relationship of these variables was expected to be weakened. As emerging evidence has suggested that intratumoral heterogeneity is associated with the malignancy diagnosis, survival or therapy response [36–38], our promising results reveal that intratumoral heterogeneity measured by DKI or IVIM may be helpful to improve our understanding of tumour biology and increasing the clinical applications of DKI or IVIM in the area of sinonasal oncology, especially when individualised treatment plans are required.

Our study still has some limitations. First, as proposed in previous studies, we adopted 50% as the Ki-67 LI cut-off (> 50% indicated a high level of proliferation status) [7, 8]. However, the optimal Ki-67 cut-off in clinical practice remains unclear and should be further clarified. Second, standard DWI, DKI and IVIM parameters obtained from ROI measurements could not be well correlated with fragmental histological specimens for Ki-67 immunohistochemistry on a site-to-site basis. A MR-guided biopsy may be needed to explore the correlations between imaging parameters and Ki-67 LI. Third, sinonasal malignancies are often associated with a varied Ki-67 LI and prognosis; thus, correlations of standard DWI, DKI and IVIM parameters with proliferation status in a specific sinonasal tumour should be further studied. Finally, we did not explore possible correlations between quantitative MR parameters and long-term clinical outcomes.

In summary, quantitative MR parameters, such as ADC derived from standard DWI, Dk and K derived from DKI together with *D* and *f* derived from IVIM, were significantly associated with Ki-67 proliferation status in patients with sinonasal malignancies. In particular, a high K_{max} value was the strongest independent indicator of a high Ki-67 proliferation status.

Funding This study has received funding from the Grant of Science and Technology Commission of Shanghai Municipality (no. 17411962100; 14411962000) and Shanghai Municipal Commission of Health and Family Planning (grant no. ZK2015A05).

Compliance with ethical standards

Guarantor The scientific guarantor of this publication is Prof. Zuohua Tang, MD, PhD, Eye and ENT Hospital of Shanghai Medical School, Fudan University, and Prof. Jinwei Qiang, MD, PhD, Jinshan Hospital of Shanghai Medical School, Fudan University.

Conflict of interest The authors of this manuscript declare no relationships with any companies, whose products or services may be related to the subject matter of the article.

Statistics and biometry No complex statistical methods were necessary for this paper.

Ethical approval Institutional Review Board approval was obtained.

Informed consent Written informed consent was waived by the Institutional Review Board.

Methodology
- retrospective
- diagnostic or prognostic study
- performed at one institution

References

1. Slootweg PJ, Ferlito A, Cardesa A et al (2013) Sinonasal tumors: a clinicopathologic update of selected tumors. Eur Arch Otorhinolaryngol 270:5–20
2. Su SY, Kupferman ME, DeMonte F et al (2014) Endoscopic resection of sinonasal cancers. Curr Oncol Rep 16:369
3. Eggesbo HB (2012) Imaging of sinonasal tumours. Cancer Imaging 12:136–152
4. Koeller KK (2016) Radiologic features of sinonasal tumors. Head Neck Pathol 10:1–12
5. Dulguerov P, Jacobsen MS, Allal AS, Lehmann W, Calcaterra T (2001) Nasal and paranasal sinus carcinoma: are we making progress? A series of 220 patients and a systematic review. Cancer 92: 3012–3029
6. Bhattacharyya N (2002) Cancer of the nasal cavity: survival and factors influencing prognosis. Arch Otolaryngol Head Neck Surg 128:1079–1083
7. Valente G, Mamo C, Bena A et al (2006) Prognostic significance of microvessel density and vascular endothelial growth factor expression in sinonasal carcinomas. Hum Pathol 37:391–400
8. Airoldi M, Garzaro M, Valente G et al (2009) Clinical and biological prognostic factors in 179 cases with sinonasal carcinoma treated in the Italian Piedmont region. Oncology 76:262–269
9. Chen WJ, He DS, Tang RX, Ren FH, Chen G (2015) Ki-67 is a valuable prognostic factor in gliomas: evidence from a systematic review and meta-analysis. Asian Pac J Cancer Prev 16:411–420
10. Stathopoulos GP, Malamos NA, Markopoulos C et al (2014) The role of Ki-67 in the proliferation and prognosis of breast cancer molecular classification subtypes. Anticancer Drugs 25:950–957
11. Fukushima S, Sugita Y, Niino D, Mihashi H, Ohshima K (2012) Clincopathological analysis of olfactory neuroblastoma. Brain Tumor Pathol 29:207–215
12. Le Bihan D (1995) Molecular diffusion, tissue microdynamics and microstructure. NMR Biomed 8:375–386
13. Yan R, Haopeng P, Xiaoyuan F et al (2016) Non-Gaussian diffusion MR imaging of glioma: comparisons of multiple diffusion parameters and correlation with histologic grade and MIB-1 (Ki-67 labeling) index. Neuroradiology 58:121–132
14. Shin JK, Kim JY (2017) Dynamic contrast-enhanced and diffusion-weighted MRI of estrogen receptor-positive invasive breast cancers: associations between quantitative MR parameters and Ki-67 proliferation status. J Magn Reson Imaging 45:94–102
15. Li HM, Zhao SH, Qiang JW et al (2017) Diffusion kurtosis imaging for differentiating borderline from malignant epithelial ovarian tumors: a correlation with Ki-67 expression. J Magn Reson Imaging. https://doi.org/10.1002/jmri.25696

16. Driessen JP, Caldas-Magalhaes J, Janssen LM et al (2014) Diffusion-weighted MR imaging in laryngeal and hypopharyngeal carcinoma: association between apparent diffusion coefficient and histologic findings. Radiology 272:456–463
17. Yuan J, Yeung DK, Mok GS et al (2014) Non-Gaussian analysis of diffusion weighted imaging in head and neck at 3T: a pilot study in patients with nasopharyngeal carcinoma. PLoS One 9:e87024
18. Jensen JH, Helpern JA, Ramani A, Lu H, Kaczynski K (2005) Diffusional kurtosis imaging: the quantification of non-Gaussian water diffusion by means of magnetic resonance imaging. Magn Reson Med 53:1432–1440
19. Le Bihan D (1988) Intravoxel incoherent motion imaging using steady-state free precession. Magn Reson Med 7:346–351
20. Le Bihan D, Breton E, Lallemand D et al (1986) MR imaging of intravoxel incoherent motions: application to diffusion and perfusion in neurologic disorders. Radiology 161:401–407
21. Jiang JX, Tang ZH, Zhong YF, Qiang JW (2016) Diffusion kurtosis imaging for differentiating between the benign and malignant sinonasal lesions. J Magn Reson Imaging. https://doi.org/10.1002/jmri.25500
22. Sumi M, Nakamura T (2013) Head and neck tumors: assessment of perfusion-related parameters and diffusion coefficients based on the intravoxel incoherent motion model. AJNR Am J Neuroradiol 34:410–416
23. Sumi M, Nakamura T (2014) Head and neck tumours: combined MRI assessment based on IVIM and TIC analyses for the differentiation of tumors of different histological types. Eur Radiol 24:223–231
24. Sumi M, Van Cauteren M, Sumi T et al (2012) Salivary gland tumors: use of intravoxel incoherent motion MR imaging for assessment of diffusion and perfusion for the differentiation of benign from malignant tumors. Radiology 263:770–777
25. Lu Y, Jansen JF, Mazaheri Y et al (2012) Extension of the intravoxel incoherent motion model to non-Gaussian diffusion in head and neck cancer. J Magn Reson Imaging 36:1088–1096
26. Jansen JF, Stambuk HE, Koutcher JA, Shukla-Dave A (2010) Non-Gaussian analysis of diffusion-weighted MR imaging in head and neck squamous cell carcinoma: a feasibility study. AJNR Am J Neuroradiol 31:741–748
27. Sun K, Chen X, Chai W et al (2015) Breast cancer: diffusion kurtosis MR imaging-diagnostic accuracy and correlation with clinical-pathologic factors. Radiology 277:46–55
28. Le Bihan D, Turner R, MacFall JR (1989) Effects of intravoxel incoherent motions (IVIM) in steady-state free precession (SSFP) imaging: application to molecular diffusion imaging. Magn Reson Med 10:324–337
29. Marzi S, Piludu F, Vidiri A (2013) Assessment of diffusion parameters by intravoxel incoherent motion MRI in head and neck squamous cell carcinoma. NMR Biomed 26:1806–1814
30. Fujima N, Yoshida D, Sakashita T et al (2017) Prediction of the treatment outcome using intravoxel incoherent motion and diffusional kurtosis imaging in nasal or sinonasal squamous cell carcinoma patients. Eur Radiol 27:956–965
31. Fudaba H, Shimomura T, Abe T et al (2014) Comparison of multiple parameters obtained on 3T pulsed arterial spin-labeling, diffusion tensor imaging, and MRS and the Ki-67 labeling index in evaluating glioma grading. AJNR Am J Neuroradiol 35:2091–2098
32. Iima M, Le Bihan D (2016) Clinical intravoxel incoherent motion and diffusion MR imaging: past, present, and future. Radiology 278:13–32
33. Le Bihan D, Turner R (1992) The capillary network: a link between IVIM and classical perfusion. Magn Reson Med 27:171–178
34. Lewin M, Fartoux L, Vignaud A et al (2011) The diffusion-weighted imaging perfusion fraction f is a potential marker of sorafenib treatment in advanced hepatocellular carcinoma: a pilot study. Eur Radiol 21:281–290
35. Liu C, Wang K, Chan Q et al (2016) Intravoxel incoherent motion MR imaging for breast lesions: comparison and correlation with pharmacokinetic evaluation from dynamic contrast-enhanced MR imaging. Eur Radiol 26:3888–3898
36. Lai V, Lee VH, Lam KO et al (2015) Intravoxel water diffusion heterogeneity MR imaging of nasopharyngeal carcinoma using stretched exponential diffusion model. Eur Radiol 25:1708–1713
37. Parikh J, Selmi M, Charles-Edwards G et al (2014) Changes in primary breast cancer heterogeneity may augment midtreatment MR imaging assessment of response to neoadjuvant chemotherapy. Radiology 272:100–112
38. Yoon SH, Park CM, Park SJ et al (2016) Tumor heterogeneity in lung cancer: assessment with dynamic contrast-enhanced MR imaging. Radiology 280:940–948